UNIVERSITY OF LEEDS

This is a repository copy of *The interaction between mixture components in the mechanism of binary fluidization*.

White Rose Research Online URL for this paper:
http://eprints.whiterose.ac.uk/104484/

Version: Accepted Version

White Rose
university consortium
Universities of Leeds, Sheffield & York

eprints@whiterose.ac.uk
https://eprints.whiterose.ac.uk/

THE INTERACTION BETWEEN MIXTURE COMPONENTS

IN THE MECHANISM OF BINARY FLUIDIZATION

B. Formisani*, R. Girimonte and V. Vivacqua

Department of Environmental and Chemical Engineering,

University of Calabria, I 87030 Arcavacata di Rende (Cosenza), Italy

*Correspondind author. Tel: +39 0984 496691; fax: +39 0984 496655.
 E-mail address: bruno.formisani@unical.it

Abstract

The interaction between components during segregating fluidization of two-solid mixtures is shown to be an intrinsic feature of their mechanism of suspension. Separate force balances on either mixture component lead to assessing the individual contribution of the two solids to the total pressure drop. An analytical expression for the interaction force is thus obtained that explains why the complete fluidization of the mixture is possible at a velocity lower that the higher u_{mf} of the two components and how the roles of 'flotsam' and 'jetsam' are attributed to them during the process of segregation.

The theoretical expressions for the initial and final fluidization velocity of a binary mixture provided by this more insightful method of analysis are identical to those discussed in previous works and validated by a wide variety of experimental results.

1. Introduction and previous work

Component segregation during fluidization of multi-solid beds is considered a practically unavoidable phenomenon that often has detrimental effects on the performance of many industrial

processes based on fluid-bed technology. Segregating fluidization in beds of two solids has therefore been extensively investigated in the last four decades, but in spite of this unceasing endeavor the comprehension of its mechanism and its theoretical representation are still unsatisfactory. The frequent recourse to empiricism, typical of most literature descriptions of segregation, is the obvious consequence of the absence of a convincing theory. Important aspects still poorly understood are the mechanism by which the presence of each of the two bed components modifies the action of the fluid on the other solid and the nature of the interaction between the two particulate species during the fluidization process.

The existence of an interaction mechanism between the two solids is suggested by experiments, which show that the packed-to-fluidized bed transition of two-solid systems is not accomplished at a single velocity threshold but along a velocity interval. The characteristic boundaries of this interval, shown in Fig.1, are usually referred to as the initial and final fluidization velocity, u_{if} and u_{ff}, respectively. On the pressure drop versus gas velocity diagram, u_{if} is located at the point Δp first deviates from the fixed bed trend, whereas u_{ff} is the velocity at which the ultimate value of Δp is attained. The pioneering studies of Chen and Keairns [1], Gelperin and Einstein [2] and Vaid and Sen Gupta [3] first revealed that fluidization of binary and ternary beds is a process that has place gradually. More recently, the dependence of both u_{if} and u_{ff} on the main variables which determine the fluidization pattern (solid properties, mixture composition and bed geometry) has been investigated by Formisani et al. [4-6], who analyzed the behaviour of a large number of two-component mixtures. These studies have provided experimental evidence that the values of u_{if} and u_{ff} are located in between the minimum fluidization velocities of the system components. A rationale for this behaviour is related to the presence of a mutual interaction between the particulate species that constitute the bed: in any binary mixture one of the two solids begins to be fluidized at a velocity lower than its u_{mf}, so that it appears to benefit from the presence of the other component; on the contrary, the suspension process of the latter results hindered, as it ends at a velocity higher than its u_{mf}.

2

As discussed in this paper, clarifying the nature of this interaction requires undertaking a separate analysis of the forces that act on either mixture component. Such an approach is alternative to that traditionally followed by many authors [7-13]; in their investigations, the binary mixture subjected to fluidization is always regarded as the equivalent of a monosolid system whose particle density and size are defined by suitable averages of those of its components. These average parameters are then introduced into well-established equations devised for calculating the minimum fluidization velocity of monocomponent beds without any theoretical justification. Following this approach, quantifying the specific effect of each component on the fluidization behaviour of the mixture becomes unfeasible.

Recently, Formisani et al. [5-6] have developed a unified model of the fluidization behaviour of all types of two-solid mixtures. On showing how the existence of a fluidization velocity interval is associated to the progress of segregation, this model provides a fully theoretical equation for predicting the initial fluidization velocity of a mixture and uses only one parameter, endowed with physical meaning, to calculate its final fluidization velocity. Even if it gives a deeper insight into the nature of segregating fluidization, a limitation of the analysis conducted so far is that of being based on force balances referred to the binary bed as a whole. A necessary development, therefore, seems that presented in the present study, where separate force balances are written for either mixture component, a method that elucidates the interaction between the two solids and leads to its quantitative evaluation.

2. Theory

2.1. Single Component Force Balances

To interpret the behaviour of the two components during the fluidization process of a homogeneous binary mixture, the "separated flow model" of Wallis [14], successfully applied by the author to monosolid fluidization, can be used. The essential feature of this approach is that of

adopting a quasi-continuum representation of the two-phase system, based on the assumption that the forces acting on the different phases are calculated in an element of volume larger than the particles.

Separated force balances on each solid can thus be written as follows:

Solid 1

$$-\rho_1 g + f_{s1,f} + f_{s1,s2} = 0 \tag{1}$$

Solid 2

$$-\rho_2 g + f_{s2,f} + f_{s2,s1} = 0 \tag{2}$$

In these relationships $f_{si,f}$ represents the force exerted by the fluid on the unit volume of solid i; analogously, a term like $f_{s1,s2}$ indicates the force transferred from solid 2 to the unit volume of solid 1.

As regards the former type of interaction, the total force $F_{s,f}$ that the fluid exerts on the solids can be divided into a pure drag force F_d and a lift force due to the pressure field surrounding the particles; $F_{s,f}$ can therefore be expressed as:

$$F_{s,f} = V_s \left(-\frac{dp}{dz} \right) + f_d V_f \tag{3}$$

In eqn 3, f_d is the pure drag force per unit volume of fluid, V_f, which does not include the pressure gradient while V_s is the total volume of the solids.

The pressure drop in the fluid phase is the sum of two contributions: gravitational head loss and friction on the solid surfaces. Accordingly, with reference to the unit volume of fluid, the pressure gradient can be written as:

$$-\frac{dp}{dz} = \rho_f g + f_d \tag{4}$$

4

Thus, in order to obtain the expression of the interaction force it is necessary to assess the contribution of the individual solid components to the "frictional pressure drop" f_d.

2.2. Drag force on single components

As with other frictional phenomena, f_d can be expressed by a relationship that expresses its dependence on the kinetic energy of the fluid as well as on system geometry by defining a suitable drag coefficient:

$$f_d = C'_D \frac{1}{2} \rho_f v^2 \frac{A}{V_f}$$

(5)

in it A and V_f are the external surface of the particles and the gas volume in the bed, respectively. This formulation has been shown by Wallis [14] to provide a theoretical basis to Carman-Kozeny's or Ergun's equation and is here adapted to the case of a homogeneous bed of two solids; to do that, one has to distinguish the contribution of either component to the total pressure drop:

$$f_d = C'_D \frac{1}{2} \rho_f v^2 \left(\frac{A_1}{V_f} + \frac{A_2}{V_f} \right)$$

(6)

With the assumption that component concentrations and bed voidage are uniform throughout the bed, the external surface of the two solids can be expressed as follows:

$$\frac{A_1}{V_f} = \frac{x_1 (1-\varepsilon)/\varepsilon}{\pi d_1^3/6} \pi d_1^2 = \frac{6 x_1 (1-\varepsilon)}{d_1 \varepsilon}; \quad \frac{A_2}{V_f} = \frac{x_2 (1-\varepsilon)/\varepsilon}{\pi d_2^3/6} \pi d_2^2 = \frac{6 x_2 (1-\varepsilon)}{d_2 \varepsilon}$$

(7)

Substitution of eqns (7) into (6) and definition of a new friction factor $C_D=3C_D'/2$ yield:

$$f_d = 2C_D \rho_f u^2 \frac{1-\varepsilon}{\varepsilon^3}\left(\frac{x_1}{d_1} + \frac{x_2}{d_2}\right)$$

(8)

In eqn (8) u is the superficial fluid velocity, related to the interstitial fluid velocity by the expression:

$$v = \frac{u}{\varepsilon}$$

(9)

As regards the dependence of the friction coefficient C_D on Reynolds number, Wallis theory of monosolid fluidization makes use of the following definition:

$$Re = \frac{\rho_f v V_f / A}{\mu_f}$$

(10)

It seems therefore appropriated, when dealing with a mixture of two solids, to change the geometric factor V_f/A into $V_f/(A_1+A_2)$, so that neglecting the factor 6 (that only changes the numerical value of Re) allows writing

$$Re = \frac{\rho_f v V_f}{(A_1 + A_2)\mu_f} = \frac{\rho_f \cdot u}{\mu_f(1-\varepsilon)}\left(\frac{x_1}{d_1} + \frac{x_2}{d_2}\right)^{-1}$$

(11)

The same author showed that the relationship

$$C_D = \frac{90}{Re}$$

(12)

6

converts eqn (6) into the classical form of Carman-Kozeny; thus, as far as it holds also for a two-component bed, substitution of eqns (9) and (12) into eqn (8) leads to the following relationship:

$$f_d = 180 \mu_f u \frac{(1-\varepsilon)^2}{\varepsilon^3 d_{av}} \left(\frac{x_1}{d_1} + \frac{x_2}{d_2} \right) \tag{13}$$

In eqn (13) d_{av} is the Sauter mean diameter of the particle assembly, defined by the relationship

$$\frac{1}{d_{av}} = \frac{x_1}{d_1} + \frac{x_2}{d_2} \tag{14}$$

so that eqn (13) can also be written as

$$f_d = 180 \mu_f u \frac{(1-\varepsilon)^2}{\varepsilon^3 d_{av}^2} \tag{13'}$$

The meaning of eqn (13) is that the pressure drop to which the gas phase is subjected while flowing across the two-component bed is the sum of the contributions of either solid, to be calculated separately as:

$$f_{d,s1} = 180 \, \mu_f u \frac{(1-\varepsilon)^2}{\varepsilon^3 \, d_{av}} \frac{x_1}{d_1} \tag{15}$$

$$f_{d,s2} = 180 \, \mu_f u \frac{(1-\varepsilon)^2}{\varepsilon^3 \, d_{av}} \frac{x_2}{d_2} \tag{15'}$$

Thus, the contribution of each mixture component to the total pressure drop turns up to be assessed by the two terms

$$\frac{x_1 d_{av}}{d_1} \qquad \text{and} \qquad \frac{x_2 d_{av}}{d_2} \quad ,$$

which coincide, respectively, with the surface fractions $A_1/(A_1+A_2)$ and $A_2/(A_1+A_2)$ and are therefore related to the relative abundance of either component in the binary mixture.

An analogous result is obtained when Ergun's equation (or any other relationship of the same kind) is used in place of Carman-Kozeny's, the only difference being that the dependence of the friction factor on Reynolds number, previously given by eqn (12), is now expressed by the relationship

$$C_D = \frac{75}{Re} + 0.875 \tag{16}$$

When the friction factor is that provided by eqn (16), the individual contribution of either mixture component to the total pressure drop per unit bed height becomes

$$f_{d,si} = 150\,\mu_f u\,\frac{(1-\varepsilon)^2}{\varepsilon^3\,d_{av}}\,\frac{x_i}{d_i} + 1.75\,\rho_f\,u^2\,\frac{(1-\varepsilon)}{\varepsilon^3\,d_{av}}\,\frac{x_i}{d_i} \tag{17}$$

while the total pressure drop is accordingly calculated as

$$f_d = 150\mu_f u\,\frac{(1-\varepsilon)^2}{\varepsilon^3 d_{av}^2} + 1.75\rho_f u^2\,\frac{(1-\varepsilon)}{\varepsilon^3 d_{av}} \tag{18}$$

3. Interaction forces between mixture components

According to what illustrated in the previous section, assessing the contribution of either mixture component to the overall pressure drop requires assuming the two component surface fractions as

the right partition factors. Consistently, the force that the fluid exchanges with the single solid component can be calculated by adapting eqn (3) to the presence of the two mixture components:

$$F_{si,f} = V_{si}\left(-\frac{dp}{dz}\right) + f_d \frac{x_i d_{av}}{d_i} V_f \tag{19}$$

The force per unit volume of solid i, $f_{si,f}$, is:

$$f_{si,f} = \frac{F_{si,f}}{V_{si}} = \left(-\frac{dp}{dz}\right) + f_d \frac{d_{av}}{d_i} \frac{\varepsilon}{(1-\varepsilon)} \tag{20}$$

Substitution of eqns (4) and (13) into (20) then yields:

$$f_{si,f} = \rho_f g + 180 \frac{\mu_f u}{d_{av}^2} \frac{(1-\varepsilon)}{\varepsilon^3}\left[(1-\varepsilon) + \varepsilon \frac{d_{av}}{d_i}\right] \tag{21}$$

Eqn (21) is then introduced into eqns (1) and (2) to obtain:

Solid 1
$$-\rho_1 g + \rho_f g + 180 \frac{\mu_f u}{d_{av}^2} \frac{(1-\varepsilon)}{\varepsilon^3}\left[(1-\varepsilon) + \varepsilon \frac{d_{av}}{d_1}\right] + f_{s1,s2} = 0 \tag{22}$$

Solid 2
$$-\rho_2 g + \rho_f g + 180 \frac{\mu_f u}{d_{av}^2} \frac{(1-\varepsilon)}{\varepsilon^3}\left[(1-\varepsilon) + \varepsilon \frac{d_{av}}{d_2}\right] - f_{s1,s2} \frac{x_1}{x_2} = 0 \tag{23}$$

where the mutual force exchange between the two solids has also been considered:

$$f_{s1,s2} x_1 = -f_{s2,s1} x_2 \tag{24}$$

Eqns (22) and (23) can be solved to obtain the expressions of the two unknowns u and $f_{s1,s2}$:

$$u = \frac{\left[(\rho_1 x_1 + \rho_2 x_2) - \rho_f\right]g d_{av}^2 \varepsilon^3}{180 \mu_f (1 - \varepsilon)} \tag{25}$$

$$f_{s1,s2} = (\rho_1 - \rho_f)g - \left[(\rho_1 x_1 + \rho_2 x_2) - \rho_f\right]g\left[(1 - \varepsilon) + \varepsilon \frac{d_{av}}{d_1}\right] \tag{26}$$

Finally, the total pressure drop per unit bed height can be calculated from eqns (4), (13) and (25) as:

$$-\frac{dp}{dz} = -\frac{\Delta p}{H} = g\left[\rho_f \varepsilon + (1 - \varepsilon)(\rho_1 x_1 + \rho_2 x_2)\right] \tag{27}$$

In the previous analysis, the interaction force expressed by eqn (26) has been derived under the assumption of viscous regime. However, an identical result can be obtained in the inertial regime. To this purpose, eqn (18) is used instead of eqn (13) in the component force balances, yielding:

Solid 1
$$-\rho_1 g + \rho_f g + \left[150 \frac{\mu_f u}{d_{av}^2} \frac{(1 - \varepsilon)}{\varepsilon^3} + 1.75 \frac{\rho_f u^2}{\varepsilon^3 d_{av}}\right]\left[(1 - \varepsilon) + \varepsilon \frac{d_{av}}{d_1}\right] + f_{s1,s2} = 0 \tag{28}$$

Solid 2
$$-\rho_2 g + \rho_f g + \left[150 \frac{\mu_f u}{d_{av}^2} \frac{(1 - \varepsilon)}{\varepsilon^3} + 1.75 \frac{\rho_f u^2}{\varepsilon^3 d_{av}}\right]\left[(1 - \varepsilon) + \varepsilon \frac{d_{av}}{d_2}\right] - f_{s1,s2} \frac{x_1}{x_2} = 0 \tag{29}$$

Multiplying eqns (28) and (29) by x_1 and x_2, respectively, and adding them together gives an equation for the calculation of the equilibrium velocity u at high Reynolds numbers:

$$150 \frac{\mu_f u}{d_{av}^2} \frac{(1 - \varepsilon)}{\varepsilon^3} + 1.75 \frac{\rho_f u^2}{\varepsilon^3 d_{av}} = \left[(\rho_1 x_1 + \rho_2 x_2) - \rho_f\right]g \tag{30}$$

Combination of eqn (30) with eqn (28) gives the same result for the interaction force as in the case of the viscous regime, i.e.:

10

$$f_{s1,s2} = (\rho_1 - \rho_f)g - [(\rho_1 x_1 + \rho_2 x_2) - \rho_f]g\left[(1-\varepsilon) + \varepsilon\frac{d_{av}}{d_1}\right] \qquad (31)$$

4. Results and discussion

Equations (25)-(27) constitute the basis of a fundamental model of binary fluidization developed as a modified version of that in use for monosolid systems. Their analytical form illustrates how the force equilibrium typical of the incipient fluidized state is influenced by mixture composition and bed voidage. However, as these two variables cease to be uniform throughout the bed as soon as particle fluidization begins, the velocity calculated by eqn (25) is but the "initial fluidization velocity" u_{if} of the homogeneous two-solid mixture.

Right after the commencement of the phenomenon, segregation begins to alter the axial distribution of the two components as well as the local voidage and the mutual interaction force. This leads to the formation of stratified layers in which the volume fraction of one of the two solids grows higher than its average value in the whole system while that of the other becomes lower. With the variation of ε and $f_{s1,s2}$, the typical issue is that at u_{if} the formation of a bubbling layer occurs together with that of a defluidized stratum. A velocity increase is then needed to restore the fluidization equilibrium in a larger portion of the bed until, at u_{ff}, all the mixture is suspended. However, although eqns (21)-(23) should hold all over the velocity interval of fluidization, calculation of u_{ff} is impeded by the fact that x_1, x_2, ε and other parameters, whose local values are determined by the extent of segregation past u_{if}, are no more uniform along the bed height.

In spite of these limitations, imposed by the persisting difficulty of relating the progress of segregation to that of fluidization, the theoretical results obtained apparently give a deeper insight into several aspects of the dynamics of multicomponent fluidization.

4.1 Effects of the interaction between components on the mechanism of binary fluidization

The method of analysis adopted in this work, which consists of writing separate force balances on the individual mixture components, has been shown to lead to the theoretical expression of the initial fluidization velocity embodied by eqn (25). This relationship is formally identical to that obtained by a different approach and validated by experimental results relevant to a large number of two-solid systems [4-6], so that no further check of its accuracy (easily recognizable in the figures of this section) is here required. More interesting is that the present investigation provides a better understanding of the mechanism by which in any mixture of two solids one of the two components enters the suspended state at a velocity higher than its u_{mf}, whereas the other achieves fluidization at u_{ff}, a velocity however lower than its u_{mf}. These circumstances, first highlighted by Chen and Keairns [1] and Vaid and Sen-Gupta [3], find now a convincing explanation, so as to allow a quantitative interpretation.

According to what sketched in Fig.2, where component 1 is assumed to be that having the lower u_{mf} (sometimes indicated as the "fluidized" component), the force $f_{s2,s1}$ arises when the gas drag and the action of the pressure field acting on solid 1 exceed its weight, so that the unbalanced excess of force is transferred to the other component. In opposition to that, component 2 (i.e. the "packed" one), whose weight is not yet balanced by the combined action of the fluid drag and the pressure field, transfers to solid 1 an additional force directed downwards, which hinders the suspension of this component. Given the expression of the interaction force provided by eqn (26), $f_{s1,s2}$ (i.e. the force exerted by solid 2 on solid 1) results positive when directed upwards.

Comparing the variation of the interaction force between components with that of the initial fluidization velocity of the binary mixture demonstrates the key-role played by this force on the overall system behaviour. To illustrate the properties of more and more complicated systems, several couples of diagrams will thus be considered; in each of them the experimental trend of $u_{if}-u_{mf,1}$ versus x_1 as well as the theoretical curve drawn from eqn (25) are compared with that of $-f_{s1,s2}$. The velocity difference taken into account represents the amount by which fluidization of component 1 (i.e. that having the lower u_{mf}) is delayed when it finds itself uniformly mixed with the solid 2 in a given proportion. On the other hand, $f_{s1,s2}$ represents the force exerted on solid 1 by

solid 2; this force is in almost all cases directed downwards so that changing its sign is just a way of highlighting the similarity between the variables under consideration.

The properties of the experimental solids which form the systems relevant to Figs 2-6 are reported in Table 1. The dependence of the voidage of the homogeneous mixtures on composition is provided elsewhere [5-6, 15]. Fig.3 reports the case of a mixture whose components differ only in density, their average diameter being the same. For systems of this kind, substitution of the condition $d_{av}=d_1$ into eqn (26) yields

$$f_{s1,s2} = (\rho_1 - \rho_2)x_2 g \tag{32}$$

so that the curve of $f_{s1,s2}$ reverts to the simple form of a straight line, just like that of $u_{if}\text{-}u_{mf,1}$.

The other simple case is that of a binary bed made of two cuts of the same solid, so that $\rho_1=\rho_2=\rho$. If so, eqn (26) becomes after some algebraic manipulations:

$$f_{s1,s2} = (\rho - \rho_f)d_{av}\varepsilon\left(\frac{1}{d_2} - \frac{1}{d_1}\right)x_2 g \tag{33}$$

The variation of $f_{s1,s2}$ with x_1 is compared with that of $u_{if}\text{-}u_{mf,1}$ in Fig.4. In order to clarify the effect of the voidage variation occurring in the bed at varying composition, two curves have been reported together with the experimental data of the velocity difference: the solid one is the plot of eqn (25), which fully accounts for the dependence of ε on x_1 and therefore fits the results rather accurately; the dashed curve, instead, is fictitious in that at all values of x_1 bed voidage is taken equal to ε_1 (i.e. to that of component 1 alone). Keeping ε unchanged while x_1 varies causes the trend of $u_{if}\text{-}u_{mf,1}$ versus x_1 to be very similar to that of $\text{-}f_{s1,s2}$. The reason is that the dependence of the initial fluidization velocity of the mixture on composition, expressed by eqn (25), embeds two distinct phenomena: one is the force associated to component interaction, which delays the beginning of bed suspension, while the other is the increase of the interstitial gas velocity that corresponds to the voidage reduction typical of the presence of two solids of different size in the same bed. For

this reason, even in the absence of any interaction between the two solids, any voidage reduction ends up with increasing the interstitial gas velocity, lowering by this way the superficial velocity at which the fluidization process begins. So, disregarding the dependence of ε on mixture composition is the way of highlighting the link between the component interaction force and the velocity at which the fluidization process would start without the added effect of the drag increase due to the variation of the interstitial gas velocity.

Once that the effects of density and size diversity between mixture components have been addressed, the same analysis can be extended to more complicated cases. To this regard, Figs 5 and 6 illustrate the behaviour of two mixtures constituted by solids differing both in density and size. The two beds have in common one of the two components (CE376) but the choice of the other solid is aimed to induce a substantial difference in system behaviour. In the GB271-CE376 mixture the denser solid is also the coarser, so that the difference of density between components adds itself to the difference of size in determining the tendency to segregation. On the contrary, in SS170-CE376 the denser species is the smaller, in a way that the difference of density acts in opposition to the difference of size.

As already done for the mixture GB172-GB499, two prediction curves are reported in the velocity diagrams, to isolate the effect of voidage variation on the component interaction force. It can be observed, however, that in the case of the mixture GB271-CE376, whose size ratio of 1.39 is not too high, the variation of the internal gas velocity is not too significant, so that the two trends are rather close to each other. As regards instead the fluidization properties of the binary bed SS170-CE376, the main issue is that this mixture enters the suspended state through the mechanism of "bottom fluidization", as the components with the lower u_{mf} achieves fluidization in the lower region of the column. The difference between "top" and "bottom fluidization", discussed in detail in a previous work [6], is here just sketched in Fig.7: in the former case, the commencement of fluidization occurs in the upper region of the bed, with the formation on top of it of a fluidized layer of the solid whose u_{mf} is lower; in the latter, suspension and bubbling of the

"fluidized" component are first observed in the bottom region of the bed while a packed layer of the other solid forms on top.

Consistently with this experimental finding, the curve of $-f_{s1,s2}$ results inverted with respect of that of $u_{if}-u_{mf,1}$, a circumstance that reveals how the force exerted on solid 1 by solid 2 is in this case directed upwards.

For both the types of mixture taken into consideration, the close similarity between the curves of $u_{if}-u_{mf,1}$ and those of $-f_{s1,s2}$ is evident and the role played by the component interaction force in determining the incipient suspension of the binary bed finds a new confirmation.

Even more significant is the case of a mixture like GB250-OP1544, referred to in Fig.8. This system exemplifies the behaviour of mixtures for which the mechanism of fluidization may change along with mixture composition, skipping from "top" to "bottom fluidization". In Fig.6 this change of phenomenology is signalled by the intersection of the curve of $-f_{s1,s2}$ with the x_1 axis. Olive pits are the only non-spherical particles used in this work, so that application of model equations to this mixture requires calculating its Sauter mean diameter from the following modified form of eqn (14):

$$\frac{1}{d_{av}} = \frac{x_1}{\phi_1 d_1} + \frac{x_2}{\phi_2 d_2} \tag{34}$$

Once more, the peculiar dependence on bed composition of the interaction force at work between the two components within the particulate bulk provides the explanation for a rather surprising property of the binary bed, whose fluidization process begins at its free surface as far as the value of x_1 is lower than about 0.3, or at its bottom when the volume fraction of the same component exceeds this limit.

Altogether, what observed with the various categories of mixtures investigated in this work allows stating that the mechanism by which the start of the fluidization process occurs is apparently regulated by the force exerted on the "fluidized" component by the "packed" one.

4.2 A criterion for attributing the roles of flotsam and jetsam during component segregation

Equation (26) allows also deriving a criterion to establish the segregation direction of the two components of the mixture. If the right-hand side of the relationship is positive, component 2 will exert an upward thrust on component 1, a force that will contribute to balance out its weight. This also means that component 1 will tend to sink, while component 2 will segregate in the upper region of the bed. According to the notation first introduced by Rowe et al. [16], the first component is called "jetsam", while the other is referred to as "flotsam". Thus, Eqn (26) provides a criterion to identify the flotsam as the component which satisfies the inequality:

$$\frac{\left(\rho-\rho_{\mathrm{f}}\right)}{\left(\rho_{\mathrm{av}}-\rho_{\mathrm{f}}\right)}<\left(1-\varepsilon\right)+\varepsilon\,\frac{\mathrm{d}_{\mathrm{av}}}{\mathrm{d}} \tag{35}$$

Equation (35) was first obtained by Di Maio et al. [17-18] who followed a different approach and validated this criterion by comparing its predictions with a large number of experimental data taken from the literature.

Conclusions

The theoretical analysis proposed in this work has shown that writing separate force balances for the fluid and solid constituents of a binary-solid system allows the interaction force between the two solids to emerge. Although referred to the case of well-mixed binary beds, this interaction is also present when the component concentration profile within the bed is not homogeneous. The model proposed, validated by results relevant to a wide variety of mixtures, is consistent with previous achievements and explains why the initial and the final fluidization velocities of a two-solid bed fall within the interval bounded by the minimum fluidization velocities of mixture components. Quantification of the solid-solid interaction requires specifying the drag force exerted by the fluidizing gas on the individual components of the binary bed; to this purpose, a theoretical method

is provided to evaluate the contribution of each solid to the overall pressure drop. The model also indicates the initial direction of segregation, in that it proves capable to attribute the roles of "flotsam" and "jetsam" to the components of the mixture.

Nomenclature

A	particle surface, cm^2
d	particle diameter, cm
d_{av}	Sauter mean diameter, cm
d_v	volume particle diameter (in table 1), μm
C_D, C'_D	friction factor, -
f_d	drag force per unit volume of fluid, $dyne/cm^3$
$f_{f,s1}$, $f_{f,s2}$	force per unit volume exerted on the fluid by solid 1, by solid 2, $dyne/cm^3$
$f_{s1,f}$, $f_{s1,s2}$	force per unit volume exerted on solid 1 by the fluid, by solid 2, $dyne/cm^3$
$f_{s2,f}$, $f_{s2,s1}$	force per unit volume exerted on solid 2 by the fluid, by solid 1, $dyne/cm^3$
F_d	total drag force, dyne
$F_{s,f}$	total force exerted on the solids by the fluid, dyne
g	gravity acceleration, cm/s^2
H	bed height, cm
p, Δp	pressure, pressure drop, $dyne/cm^2$
Re	Reynolds number= $\rho_f\, u\, d_{av}/[\mu_f\,(1-\varepsilon)]$, -
u_{if}, u_{ff}	initial, final fluidization velocity, cm/s
u_{mf}	minimum fluidization velocity, cm/s
v	interstitial velocity, cm/s
V_f, V_s	volume of the fluid, of the solid phase, cm^3
x	volume fraction of the solid component, -
z	vertical height, cm

Greek symbols

ε voidage, -

ϕ particle sphericity, -

μ_f fluid viscosity, g/cm s

ρ solid density, g/cm^3

ρ_{av} average density of the solid mixture (= $\rho_1 x_1 + \rho_2 x_2$), g/cm^3

ρ_f fluid density, g/cm^3

Subscripts

1   of solid 1, of the component with the lower u_{mf}

2   of solid 2, of the component with the higher u_{mf}

References

[1] Chen JL-P, Keairns DL. Particle segregation in a fluidized bed. Can. J. Chem. Eng. 1975;53:395-402.

[2] Gelperin NI, Einstein VG. The analogy between fluidized beds and liquids. In Davidson JF, Harrison D. Fluidization. London: Cambridge Press, 1978: 541-568.

[3] Vaid RP, Sen Gupta P. Minimum fluidization velocities in beds of mixed solids. Can. J. Chem. Eng. 1978;56:292-296.

[4] Formisani B, Girimonte R, Longo T. The fluidization process of binary mixtures of solids: Development of the approach based on the fluidization velocity interval. Powder Technol. 2009; 185:97-108.

[5] Formisani B, Girimonte R, Vivacqua V. Fluidization of mixtures of two solids differing in density or size. AIChE J. 2011;57:2325–2333.

[6] Formisani B, Girimonte R, Vivacqua V. Fluidization of mixtures of two solids: a unified model of the transition to the fluidized state, AIChE J. 2013;59:729-735.

[7] Goossens WRA, Dumont GL, Spaepen GL. Fluidization of binary mixtures in laminar flow region. Chem. Eng. Prog. Symp. Ser. 1971;67:38-45.

[8] Otero AR, Corella J. Fluidizacion de mezclas de solidos de distintas caracteristicas. Anales de la RSEFQ. 1971;67:1207-1219.

[9] Rowe PN, Nienow, AW. Minimum fluidization velocity of multicomponent particle mixtures, Chem. Eng. Sci. 1975;29:1365-1369.

[10] Cheung L, Nienow AW, Rowe PN. Minimum fluidization velocity of a binary mixture of different sized particles. Chem. Eng. Sci. 1974;29:1301-1303.

[11] Chiba S, Chiba T, Nienow AW, Kobayashi H. The minimum fluidization velocity, bed expansion and pressure-drop profile of binary particle mixtures, Powder Technol. 1979;22:255–269.

[12] Uchida S, Yamada H, Tada I. Minimum fluidization velocity of binary mixtures. J. Chem. Eng. 1983; 14:257-264.

[13] Thonglimp V, Hiquily N, Laguerie C. Vitesse minimale de fluidisation et expansion des couches de mélanges de particules solides fluidisées par un gaz. Powder Technol. 1984;39:223-229.

[14] Wallis GB. One-dimensional Two-phase Flow. New York: McGraw-Hill, Inc., 1969.

[15] Formisani B, Girimonte R, Vivacqua V. Modelling the transition to the fluidized state of two-solid beds: Mixtures of particles of irregular shape. In Kuipers JAM, Mudde RF, van Ommen JR, Deen NG Fluidization XIV. New York: Engineering Conference International, 2013: 243-250.

[16] Rowe PN, Nienow AW, Agbim, AJ. The mechanisms by which particles segregate in gas fluidized beds – binary systems of near spherical particles. Trans. Inst. Chem. Eng. 1972;50:310-323.

[17] Di Maio FP, Di Renzo R, Vivacqua V. A particle segregation model for gas-fluidization of binary mixtures. Powder Technol. 2012;226:180-188.

[18] Di Maio FP, Di Renzo R, Vivacqua V. Extension and validation of the particle segregation model for bubbling gas-fluidized beds of binary mixtures. Chem. Eng. Sci. 2013;97:139-151.
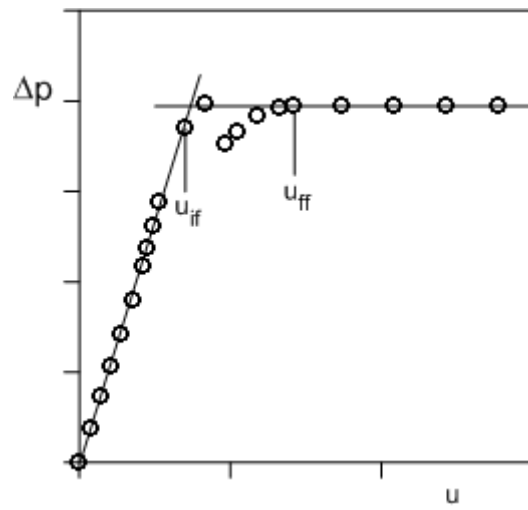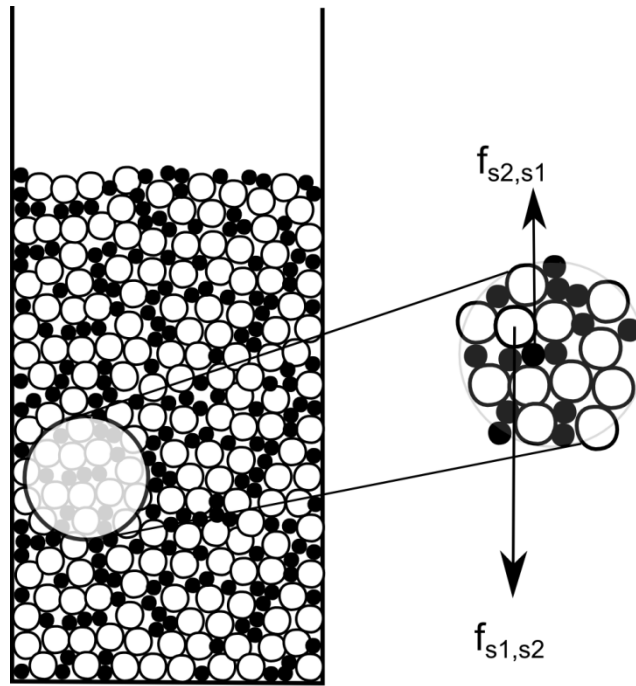
Figure 1. Boundaries of the fluidization velocity interval.

$$f_{s2,s1}$$

$$f_{s1,s2}$$

● Component s1
○ Component s2

Figure 2. The interaction between the two solids of a well-mixed binary bed.
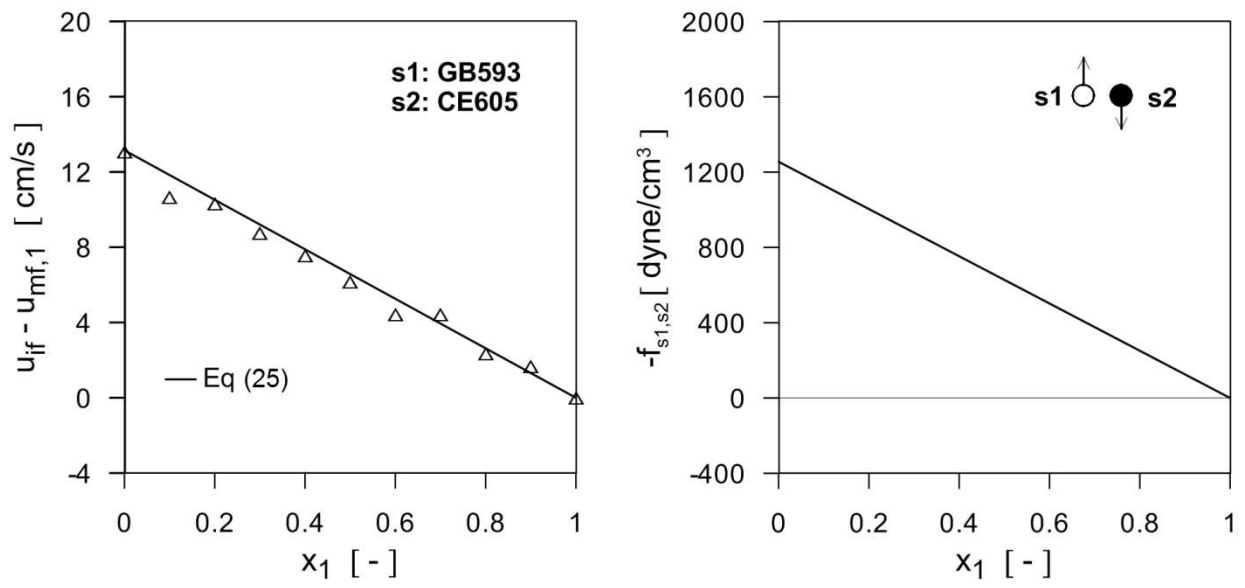
Figure 3. The relationship between onset of fluidization and interaction force between components at varying mixture composition. Solids of different density: GB593-CE605.
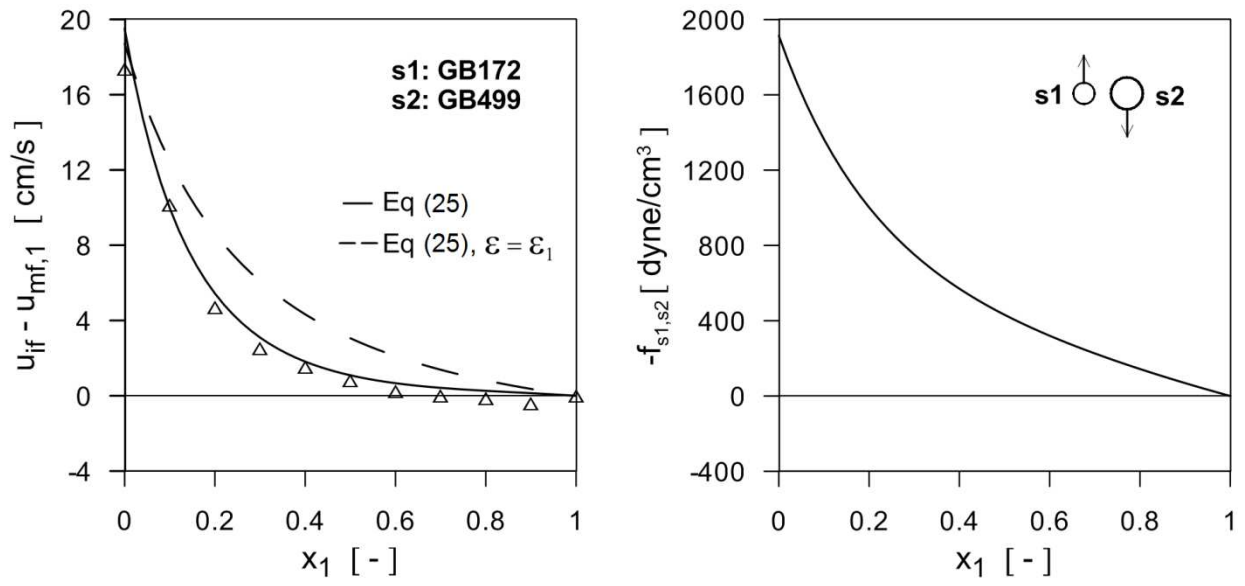
Figure 4. The relationship between onset of fluidization and interaction force between components at varying mixture composition. Solids of different size: GB172-GB499.
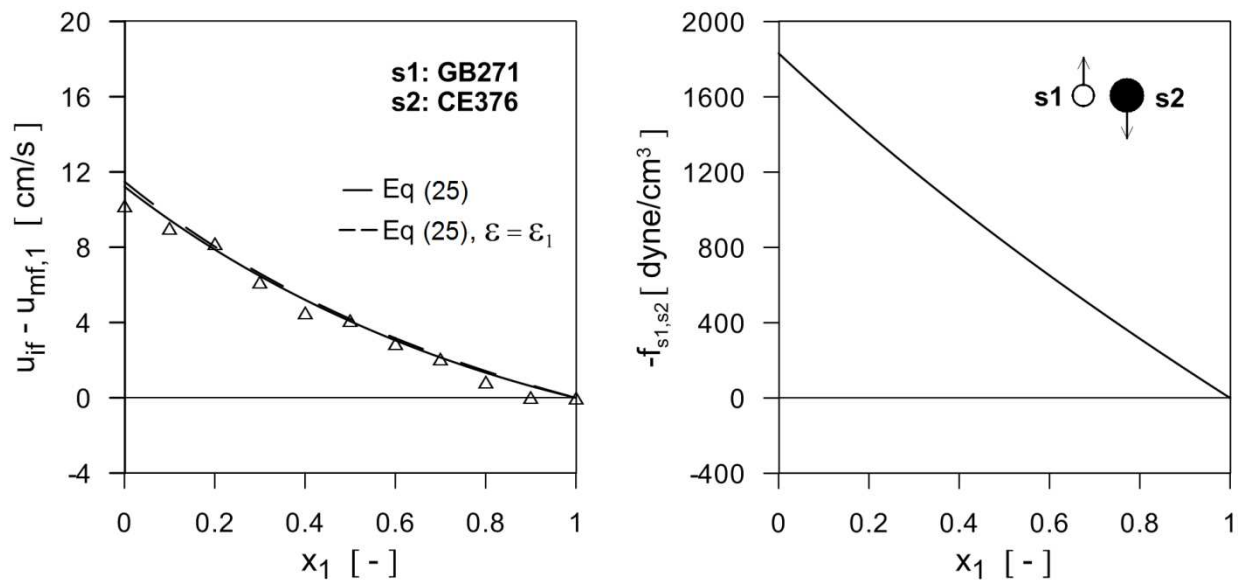
Figure 5. The relationship between onset of fluidization and interaction force between components at varying mixture composition. Dissimilar solids undergoing "top fluidization": GB271-CE376.
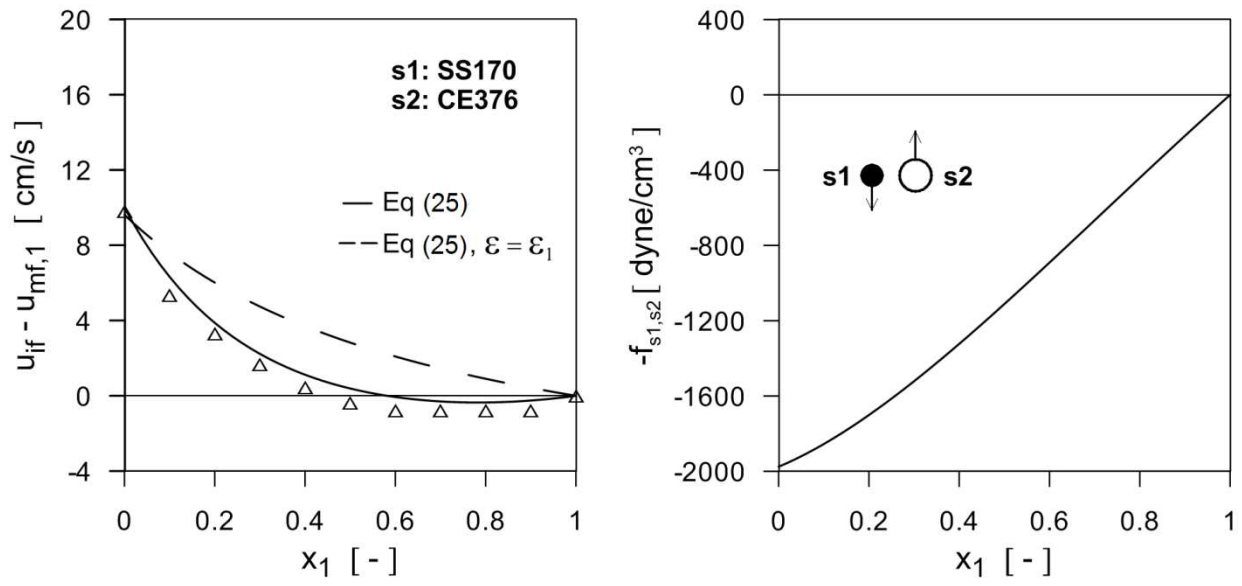
Figure 6. The relationship between onset of fluidization and interaction force between components at varying mixture composition. Dissimilar solids undergoing "bottom fluidization": SS170-CE376.
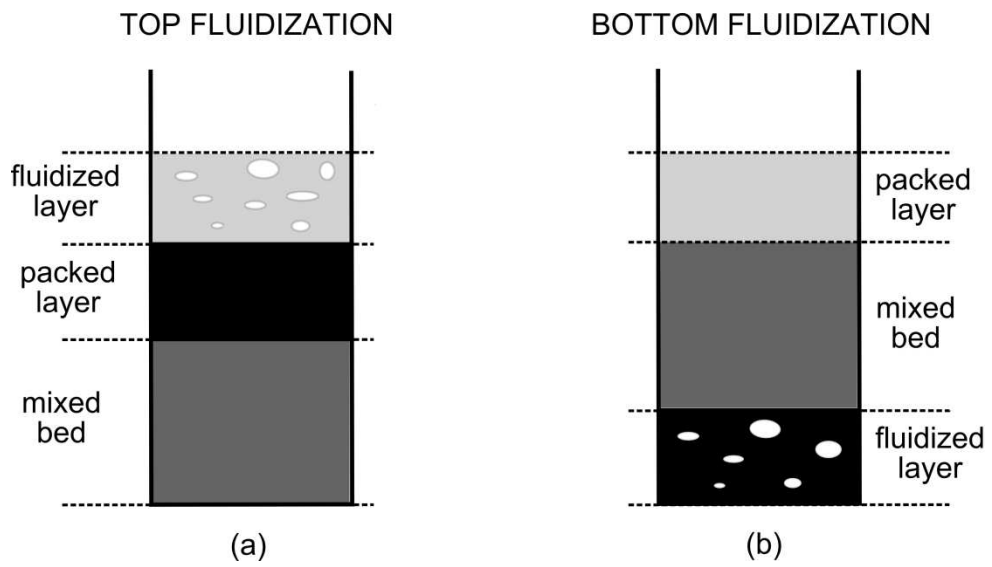
TOP FLUIDIZATION   BOTTOM FLUIDIZATION

fluidized
layer

packed
layer

mixed
bed

(a)

packed
layer

mixed
bed

fluidized
layer

(b)

Figure 7. Solid layers formed by the "top" and the "bottom fluidization" mechanisms.
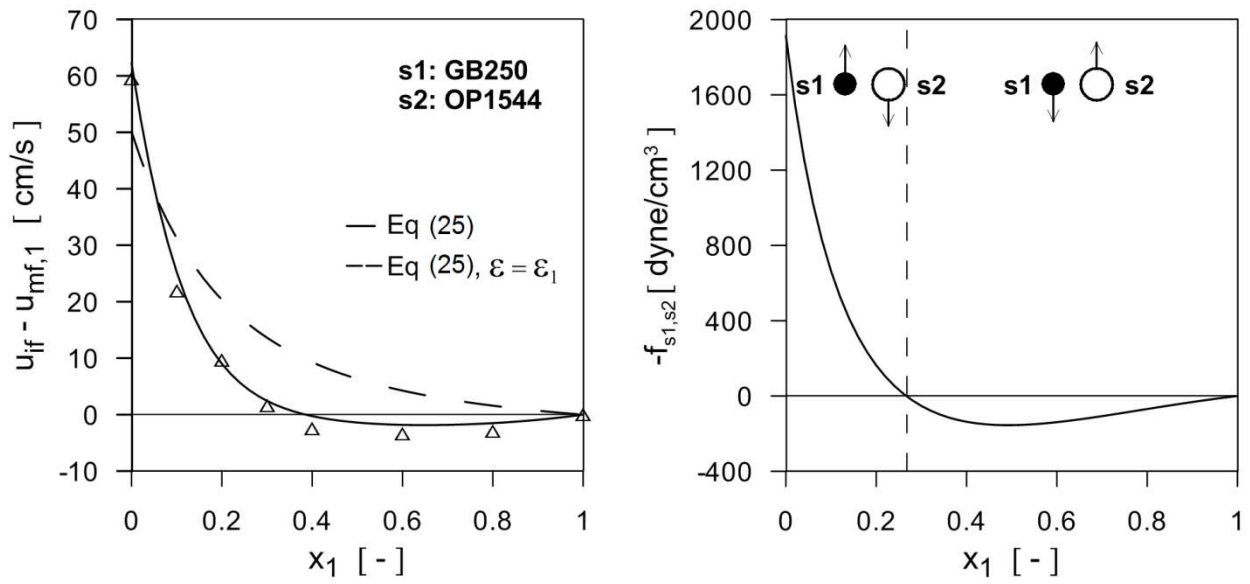
Figure 8. The relationship between onset of fluidization and interaction force between components at varying mixture composition. Dissimilar solids switching from "top" to "bottom fluidization": GB250-OP1544.

Table 1: Properties of the experimental solids.

Solid	Density [g/cm³]	Sieve size [μm]	Sauter diameter [μm]	Geldart's group	Minimum fluidization velocity [cm/s]	Re_{mf} [-]
Glass beads (GB)	2.48	150-180	172	B	2.80	0.32
		200-300	250	B	6.20	1.04
		200-300	271	B	6.50	1.18
		400-600	499	B	20.2	6.78
		500-710	593	B	30.8	12.8
Ceramic spheres (CE)	3.76	300-400	376	B	16.7	4.22
		500-710	605	B	43.3	17.6
Steel shots (SS)	7.60	150-200	170	B	6.90	0.79
Olive pits (OP)	1.38	1400-2000	1540*	D	66.1	68.4

* (ϕ=0.80; d_v=1930 μm)